LASER INTERFEROMETER GRAVITATIONAL WAVE OBSERVATORY

LIGO Laboratory / LIGO Scientific Collaboration

LIGO-T1100068-v21 *Advanced LIGO* December 2, 2014

Photon Calibrator Final Design

Jonathan Berliner, Pablo Daveloza, Rick Savage, Joe Gleason

Distribution of this document:
LIGO Scientific Collaboration

This is an internal working note
of the LIGO Laboratory.

California Institute of Technology
LIGO Laboratory, MS 100-36
Pasadena, CA 91125
Phone (626) 395-2129
Fax (626) 304-9834
E-mail: info@ligo.caltech.edu

Massachusetts Institute of Technology
LIGO Project, MIT NW22-295
185 Albany St, Cambridge, MA 02139
Phone (617) 253-4824
Fax (617) 253-7014
E-mail: info@ligo.mit.edu

LIGO Hanford Observatory
127124 North Route 10
Richland, WA 99354
Phone 509-372-8106
Fax 509-372-8137
E-mail: info@ligo.caltech.edu

LIGO Livingston Observatory
19100 LIGO Lane
Livingston, LA 70754
Phone 225-686-3100
Fax 225-686-7189
E-mail: info@ligo.caltech.edu

http://www.ligo.caltech.edu/

- **Table of Contents**

1 Introduction

1.1 Preface

This document describes the Preliminary and Final Design of the Advanced LIGO (aLIGO) Photon Calibrator subsystem ("Pcal"). It details engineering and design specifications, overall beam, hardware, and electrical layouts, as well as expected modes of operation. The design is based on the Initial LIGO (iLIGO) and Enhanced LIGO (eLIGO) Pcals. It responds to input received from the LSC Calibration Committee, mostly in the form of operational requirements.

Pcals were introduced during iLIGO principally to provide an independent check of the absolute differential length calibration (see Figure 1). During eLIGO, re-designed Pcal systems were installed in the X-end stations for both the Hanford (H1) and Livingston (L1) 4k interferometers (see Figure 2). The eLIGO Pcals operated in a two-beam configuration to minimize errors due to sensing the local elastic deformation induced by radiation pressure. The two beams were positioned on the surface of the End Test Mass (ETM) such that errors due to bulk elastic deformation of the ETM were minimized. The eLIGO Pcals incorporated internal power sensors with temperature-stabilized InGaAs photo-receivers mounted on integrating spheres.

The eLIGO Pcals operated continuously during the S6 science run, injecting a single calibration line in each interferometer with a frequency near 400 Hz. Assessment of the long-term trends in the actuator coefficients was the primary goal of the eLIGO Pcals. Analysis of the Pcal data over all of S6 revealed that the long-term (16 months) stability of the actuation coefficients of the ETM voice-coil actuators was better than 1% (p-p) for both H1 and L1. Furthermore, the Pcals were able to provide absolute calibration of the interferometers' responses. During S6, the Pcals were also used to make swept sine measurements of the interferometer closed-loop response functions over the frequency band from 70 Hz to 1 kHz.

During aLIGO, the Pcals are expected to play a more prominent role, if not the lead role, in the calibration of the LIGO interferometers. One Pcal system will be installed for each ETM, six Pcal systems in all. Upgrades for aLIGO, as detailed in this document, include more powerful lasers, more rigid support structures, and directing the beams reflected from the ETMs out of the vacuum system to continuously monitor the reflected power.

The scope of the aLIGO Pcals includes:

- Transmitter and receiver modules
- Transmitter pylon (the receiver pylon is shared with, and in the scope of, the Optical Levers subsystem)
- In-vacuum periscopes mounted on compression rings
- Gold Standard and Working Standard laser power sensor systems, including periodic absolute power calibrations at NIST, and the facility and procedures used to transfer the Gold Standard calibration to the Working Standards.
- Electronics, including laser and photo-receiver power supplies, acousto-optic modulator driver, *Optical Follower* servo for control of the modulated waveform, and analog signal conditioning filters.

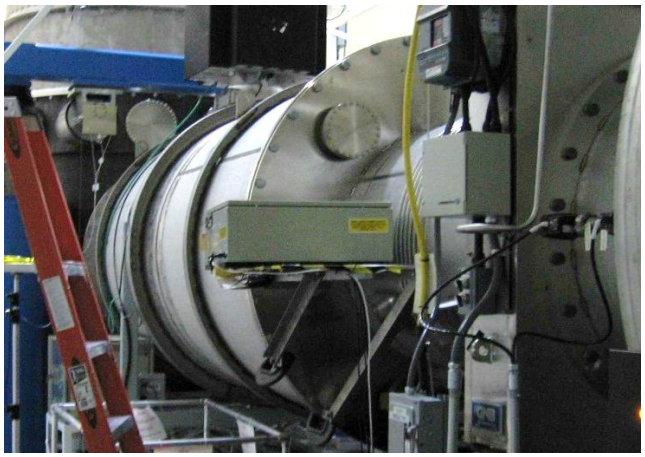

Figure 1 – iLIGO Photon Calibrator Transmitter Module

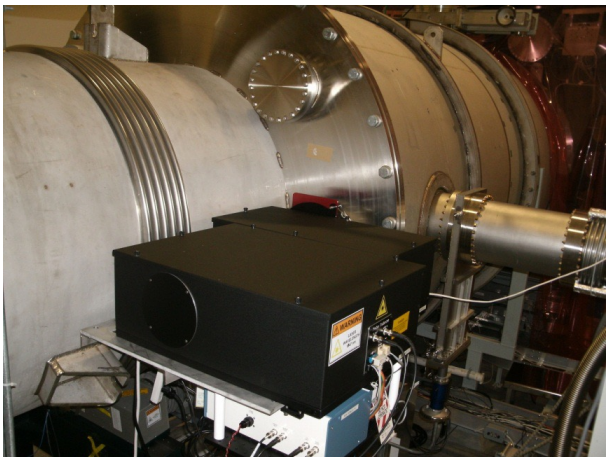

Figure 2 – eLIGO Photon Calibrator Transmitter Module

1.2 Principle of Operation

The Pcals use power-modulated auxiliary lasers to induce periodic modulations in the position of a suspended ETM via photon radiation pressure, as shown schematically in Figure 3.

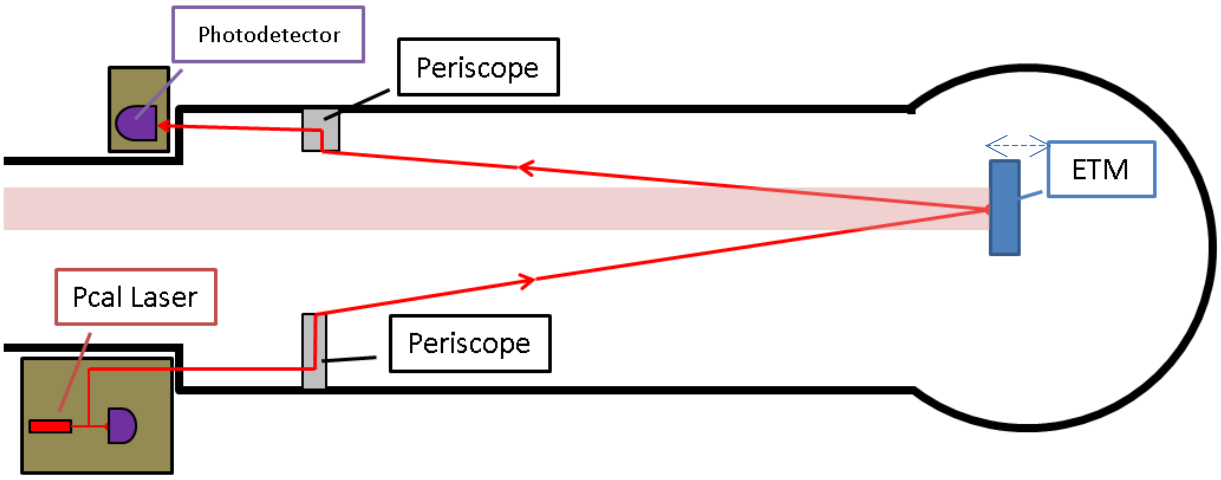

Figure 3 – Basic Schematic of aLIGO Pcal System

For modulation frequencies much higher than the ETM pendulum resonance frequency, the ETM responds as a free mass and its induced displacement is given by (1):

$$x_0 = -\frac{2p_0}{c}\frac{1}{M\omega^2}(cos\,\theta) \qquad (1)$$

where:

- x_0 is the amplitude of the periodic displacement of the ETM
- p_0 is the amplitude of the periodic laser power modulation
- c is the speed of light in vacuum

- M is the mass of the ETM
- ω is the angular frequency of the power modulation
- θ is the angle of incidence on the ETM

and the minus sign indicates that the induced displacement is 180° out of phase with the driving force.

2 Performance Requirements

This section addresses the key requirements that impact the design of the Photon Calibrators.

2.1 Accuracy of Induced Displacements: Absolute Power Calibration, Beam Positioning on ETM Surface

The sinusoidal Pcal-induced displacements of the ETMs are required to be accurate within 5% in amplitude and 16μs in timing over 2σ confidence intervals.

All of the parameters in Equation (1), except for the absolute laser power modulation amplitude, will be known with accuracies sufficient to reduce their contribution to the overall induced displacement error to below 0.1%. Equation (1) does not include contributions to sensed displacements resulting from radiation-induced rotation of the ETMs or elastic deformation of the ETMs (either local or bulk). Accurate positioning of the Pcal beams on the ETM surface can minimize both of these potential sources of calibration errors. We expect that Pcal uncertainties will be dominated by determination of absolute laser power modulation amplitudes (see Section 6). Our experience during iLIGO and eLIGO indicates that absolute laser power calibration at the 1% level (2σ) is achievable with the scheme we propose.

2.1.1 Absolute Power Calibration

Absolute laser power calibration is achieved by transferring the calibration of a *Gold Standard* power sensor that is periodically calibrated at the National Institute of Standards and Technology (NIST) to *Working Standard* power sensors that are used to calibrate power sensors that are located inside the Pcal transmitter and receiver modules, sensing the laser power directed to and reflected from the test masses.

This calibration strategy, which was developed in consultation with Dr. Joshua Hadler at NIST, is shown schematically in Figure 4. It is intended to enable "NIST traceability[1]" of the absolute power calibration of the Pcals with overall 2σ uncertainty of less than 5 percent.

[1] NIST defines traceability as "The property of the result of a measurement or the value of a standard whereby it can be related to stated references, usually national or international standards, through an unbroken chain of comparisons, all having stated uncertainties" (http://ts.nist.gov/Traceability/supplmatls/suppl_matls_for_nist_policy_rev.cfm).

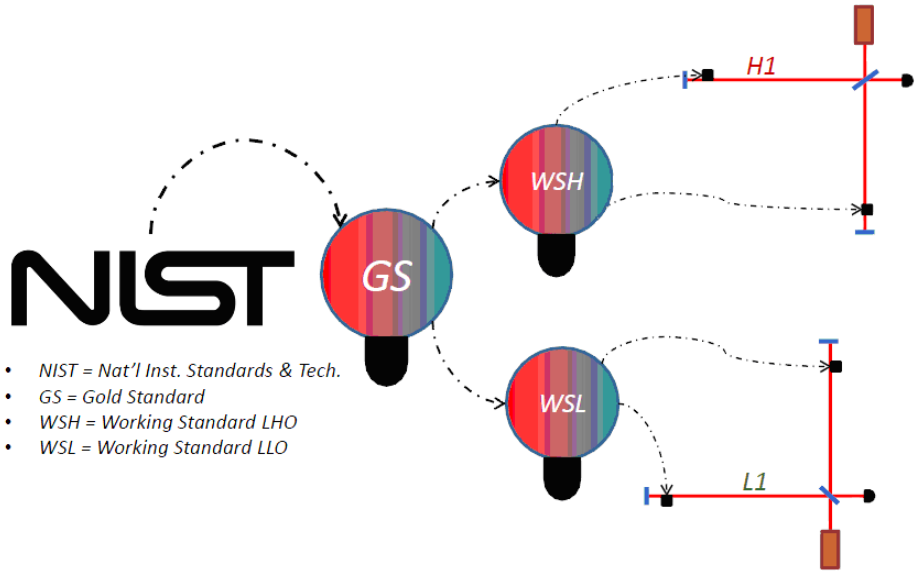

Figure 4 – aLIGO Pcal absolute laser power calibration scheme. Circles represent power calibration standards, black boxes represent Pcal transmitter modules, NIST represents the National Standard Calorimetric Calibration Facility at NIST, and dashed lines represent calibration links.

All of the aLIGO Pcal power sensors are InGaAs photoreceivers mounted on integrating spheres. While these sensors are subject to laser speckle that induces slow uncorrelated variations in their outputs (period of seconds to minutes with amplitudes of a fraction of a percent), they are insensitive to input beam parameters[2] such as alignment, divergence, polarization, spot size, etc. They have proven to be long-term stable at the 1% level. See Section 6 for a more detailed discussion of the absolute power calibration.

2.1.2 Beam Positioning on ETM Surface

To account for the impact of Pcal-induced rotation of the ETM on the displacement sensed by the interferometer, Equation (1) should be multiplied by the factor

$$\left(1 + \frac{M}{I}\vec{a} \cdot \vec{b}\right) \qquad (2)$$

where $\vec{a}$ and $\vec{b}$ are displacement vectors from the center of the face of the ETM to the center of the interferometer beam, and to the center of force for the two Pcal beams, respectively, and I is the moment of inertia about an axis through the center of the ETM and parallel to the face of the optic

[2] LIGO-T1000637

(see LIGO-P080118). Even if both displacement vectors are parallel and as large as 1 cm, the resulting factor for sensing the induced displacement, the rotational factor given by the second term of Equation (2), will be less than 0.01. This term is thus omitted from Equation (1).

Actuation forces applied to the ETMs produce both $local_{3,4}$ and $bulk_{5,6}$ elastic deformations that can significantly alter the interferometer's response, especially when the frequencies of the modulated forces are above 1 kHz. Equation (1), the Photon Calibrator displacement formula, assumes that the ETM moves as an ideal free and rigid mass. However, these elastic deformations would cause the displacement of the surface of the ETM to deviate from the ideal rigid-body motion. The aLIGO ETMs are also unique because of the flats on either side of the ETM which complicate modeling.

H. Pablo Daveloza, using Finite Element Analysis in COMSOL, studied these effects and summarized his results in LIGO-P1100166. He also investigated the optimal number of Pcal beams and the optimal locations of those beams on the surface of the ETM. The main ETM normal modes that would be excited by the Pcal radiation forces are the *butterfly* and *drumhead* modes shown Figure 5.

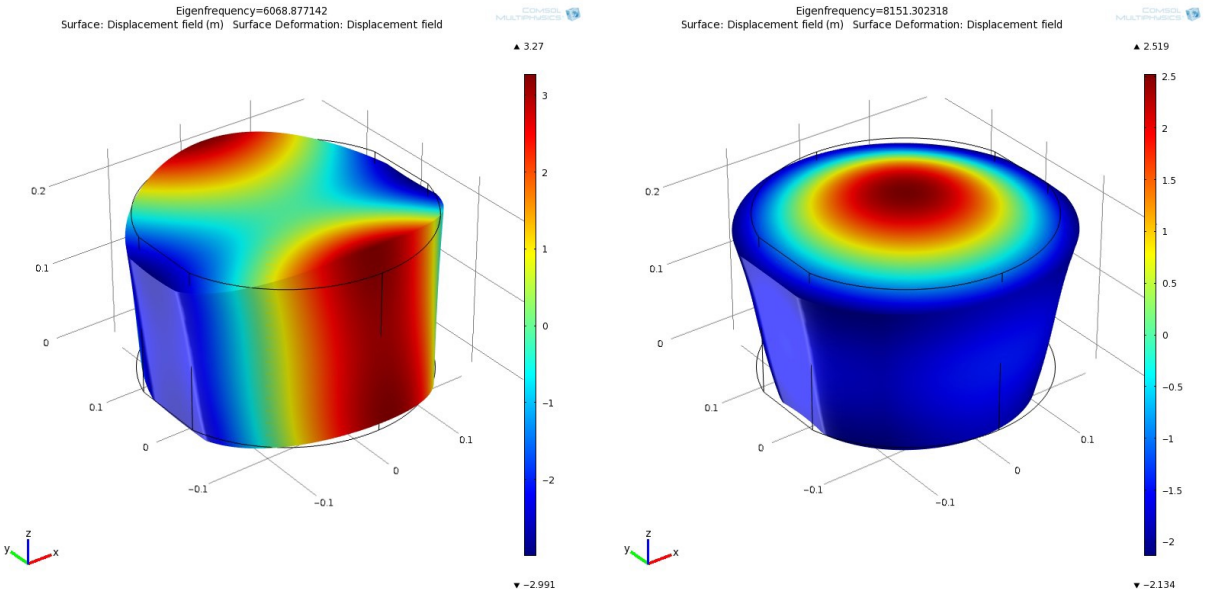

Figure 5 COMSOL simulation of the butterfly mode excited at ~6.1 kHz (left) and the drumhead mode excited at ~8.1 kHz, both for the aLIGO ETM.

The COMSOL modeling revealed that if the two Pcal beams are located optimally the excitation of the drumhead-pattern deformation of the ETM is minimized. For the aLIGO ETMs, the optimum locations are diametrically opposed and 111.6 mm from the center of the ETM as shown in Figure 6.

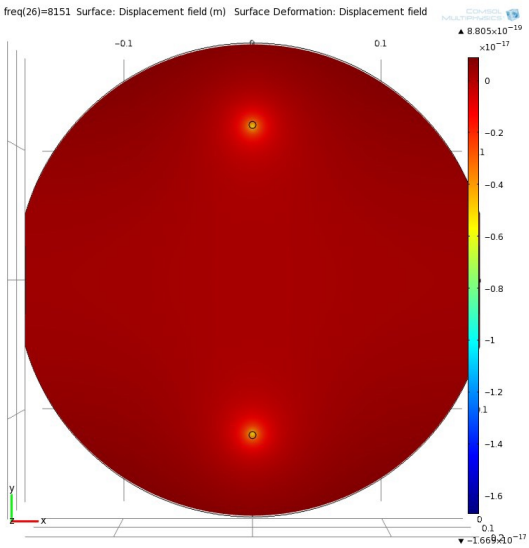

Figure 6 Ideal location of Photon Calibrator beams on ETM surface (111.6 mm from center along vertical diameter).

Optimally-located beams in 3-beam or 4-beam configurations can minimize excitation of the butterfly-pattern deformation as well. However, beam positioning constraints imposed by the folded Arm Cavity Baffles that are part of the Stray Light Control subsystem make the 3-beam and 4-beam configuration impractical. Furthermore, the FEM results showed that unless the beam locations on the ETM surface can be maintained within 1 mm of their optimal locations the 3-beam and 4-beam configurations are no better than the 2-beam configuration.

Figure 7 shows the predicted calibration errors as a function of the displacement of the Pcal beam spots from their optimum locations in a 2-beam configuration.

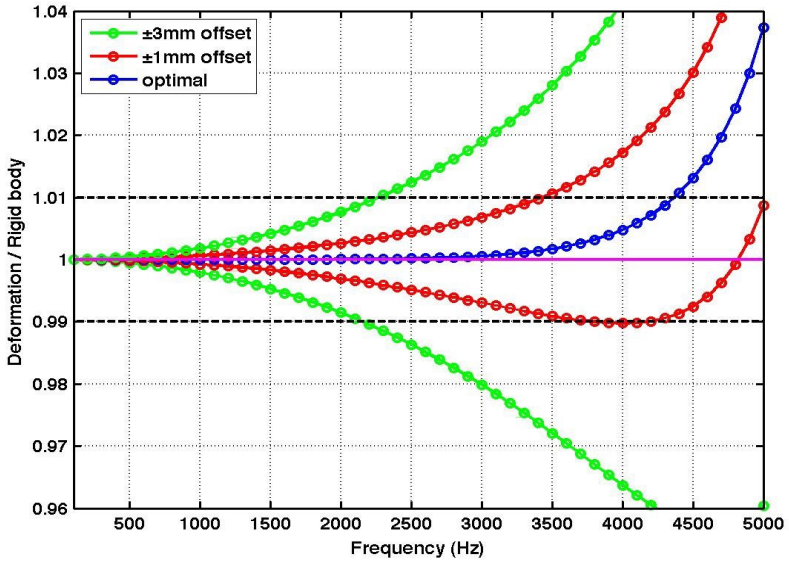

Figure 7 – Errors due to bulk elastic deformation resulting from Pcal beam spots offset from their optimal locations in the 2-beam configuration.

If the beam positions are held within 1 mm of the ideal locations, the calibration errors remain below ±1% for frequencies up to 3.5 kHz. For beam offsets up to 3 mm, the calibration errors are below ±1% up to 2 kHz. Even for optimally-located beam spots, the calibration error reaches 1% at about 4.3 kHz due to excitation of the butterfly-pattern deformation in the 2-beam Pcal configuration.

2.2 Precision of Induced Displacements: Laser Power

As shown in Equation (1), the amplitude of the modulated ETM displacement induced by the Pcals is proportional to the amplitude of the laser power modulation. The Pcals induce sinusoidally-modulated beam powers as shown in Figure 8. A conservative estimate of the amplitude (peak) of the power modulation is ¼ of the raw laser power, i.e. the peak-to-peak power modulation is half of the raw laser power. There is also an efficiency factor, ϵ, the Pcal transmitter module optical efficiency in delivering modulated laser power to the ETM. This includes the AOM diffraction efficiency of about 80% and the optical efficiency of the transmitter module optical components (polarizing beam splitter, mirrors, lenses, viewports), conservatively about 80%.

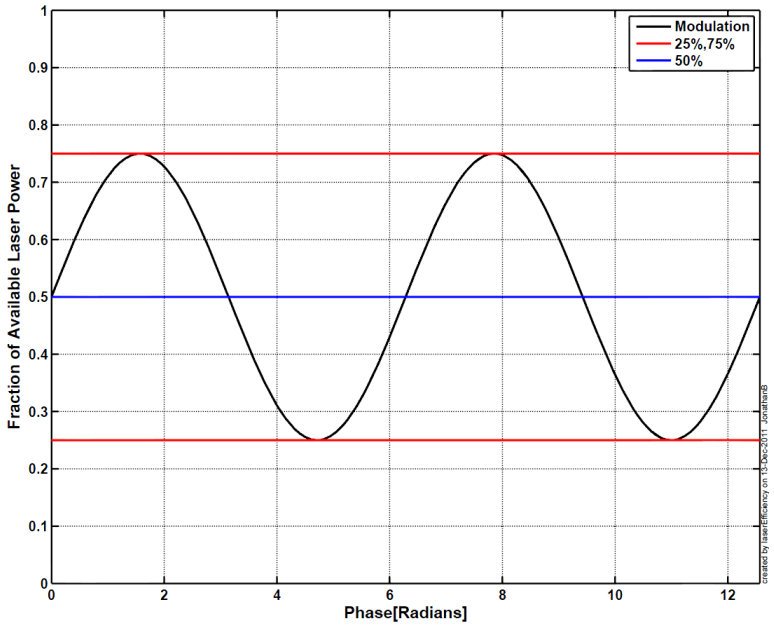

Figure 8 – Pcal power modulation as a fraction of raw laser power for 50% p-p modulation.

Using Equation (1), the total amount of raw Pcal laser power required, P_{laser}, is given by

$$P_{laser} = \sum_i \sqrt{2} L h(f_i) \frac{1}{4\epsilon} \frac{SNR(f_i)}{\sqrt{T_i}} \frac{Mc(2\pi f_i)^2}{2\cos\theta} \qquad (3)$$

where the sum is over the individual modulated displacements with index i and frequency f_i, $h(f_i)$ the is interferometer sensitivity estimate in units of strain (rms) per $\sqrt{Hz}$ (we use the "zero-detuning, high power" and "no SRM" curves published in LIGO-T0900288), the factor of $\sqrt{2}$ converts the rms strain to peak strain, L is the length of the interferometer arms, the factor of ¼ is for 50% p-p modulation as discussed above, ϵ is the transmitter module optical efficiency, $SNR(f_i)$

is the desired signal-to-noise ratio of a given reference displacement, and T_i is the length of the DFT for evaluation of a given periodic displacement.

The raw Pcal laser power required for the various reference displacements, given by Equation (3), are listed in

Table 1 in the "Pcal Laser Power" columns and shown graphically in Figure 9. The table also includes the amplitudes of the reference displacements.

Table 1 – Raw laser power requirements for Pcal reference displacements[3]

aLIGO Sensitivity Curve →			***Zero-Detuning, High Power***		***No SRM (25W Power)***	
Frequency	***DFT length***	***SNR***	***Displacement*** $(\frac{meters_{RMS}}{\sqrt{Hz}})$	***Pcal Laser Power***	***Displacement***	***Pcal Power***
50 Hz	1 second	20	4.02×10^{-19}	2.73 mW	3.99×10^{-19}	2.70 mW
400 Hz	1 second	20	3.07×10^{-19}	0.134 W	1.35×10^{-18}	0.584 W
1,100 Hz	1 second	20	4.60×10^{-19}	1.51 W	3.66×10^{-18}	12.0 W
2,000 Hz	60 second	10	3.67×10^{-19}	0.515 W	3.32×10^{-18}	4.65 W
			Total Pcal Power	***2.16 W***		***17.2 W***

Table **1** shows that as frequency increases, the required Pcal laser power increases rapidly. To maintain reasonable Pcal laser powers, the highest calibration line, which is placed beyond the UGF of the DARM servo, only requires an SNR of 10 for 60-second-long DFTs.

Note that other configurations for the Pcal excitations might also be utilized for aLIGO calibration studies. For instance, the Pcals on the two interferometer ETMs can excite excitations in differential mode, enabling twice the differential displacement excitation of a single Pcal module. Or, the two Pcal modules could operate in common mode, inducing a large common-mode excitation with minimal differential mode excitation. Observation of a peak in the differential length spectrum (or the lack thereof) would indicate a change (or lack of change) in the differential actuation of the DARM servo.

[3] Calibration SVN:
https://svn.ligo.caltech.edu/svn/calibration/trunk/calibration/frequencydomain/runs/S6/PhotonCalibrator/measurements/aLIGOstudies/rpnStudies/sensitivity.m

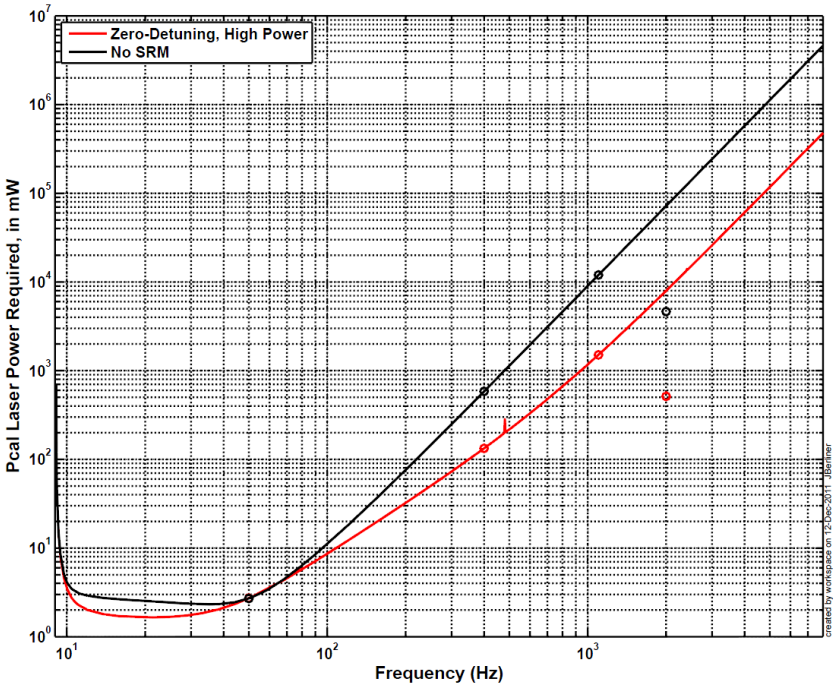

Figure 9 –Required laser power as a function of frequency for two aLIGO interferometer configurations. Circles represent reference displacements. The two circles at 2 kHz are reduced from their respective curves by $2\sqrt{60}$, reflecting their lower SNR and longer DFT time as shown in column 2 of

Table 1.

2.3 Displacement Noise: Relative Power Noise and Harmonic Noise

The amplitude spectral density of the displacement noise from Pcal, other than intentional reference displacements, shall not exceed 10% of the design sensitivity for the interferometer. We use the "zero-detuning, high power" sensitivity curve for this requirement (LIGO-T0900288).

There are two sources of displacement noise from the Pcals: inherent relative power noise from the laser (RPN) and noise introduced at harmonics of the modulation frequency due to nonlinearity of the power modulation process.

The maximum allowed displacement due to RPN is given by

$$\Delta x_{max} = 2\Delta P_{max} cos\theta/(Mc\omega^2) = Lh(f)/10 \qquad (4)$$

The average power incident on the ETM is $\epsilon P_{laser}/2$, so the maximum laser RPN is given by

$$RPN_{max} = \Delta P/(P_{laser}\epsilon/2) = \frac{Lh(f)Mc\omega^2}{10\cos\theta\, P_{laser}\epsilon} \qquad (5)$$

The maximum allowable RPN for two aLIGO sensitivity curves, the "no SRM" and the "zero-detuning, high power" configurations, assuming the raw laser powers given in

Table 1 (2.16 W and 17.2 W, respectively), are plotted in Figure 10. Also plotted for comparison are the measured RPN of two candidate lasers, a 500 mW unit sold by CrystaLaser and a 500 mW microFlare laser sold by InnoLight. Both lasers were scaled to the higher power levels assuming that the RPN of the lasers would stay the same.

The "no SRM" curve is shown for comparison only; we don't intend to procure 17 W lasers for the Pcals. Note, however, that because the Pcals will use lasers with only about 2 W output power the SNR for the Pcal reference displacement lines achievable in the "no SRM" mode will be significantly lower.

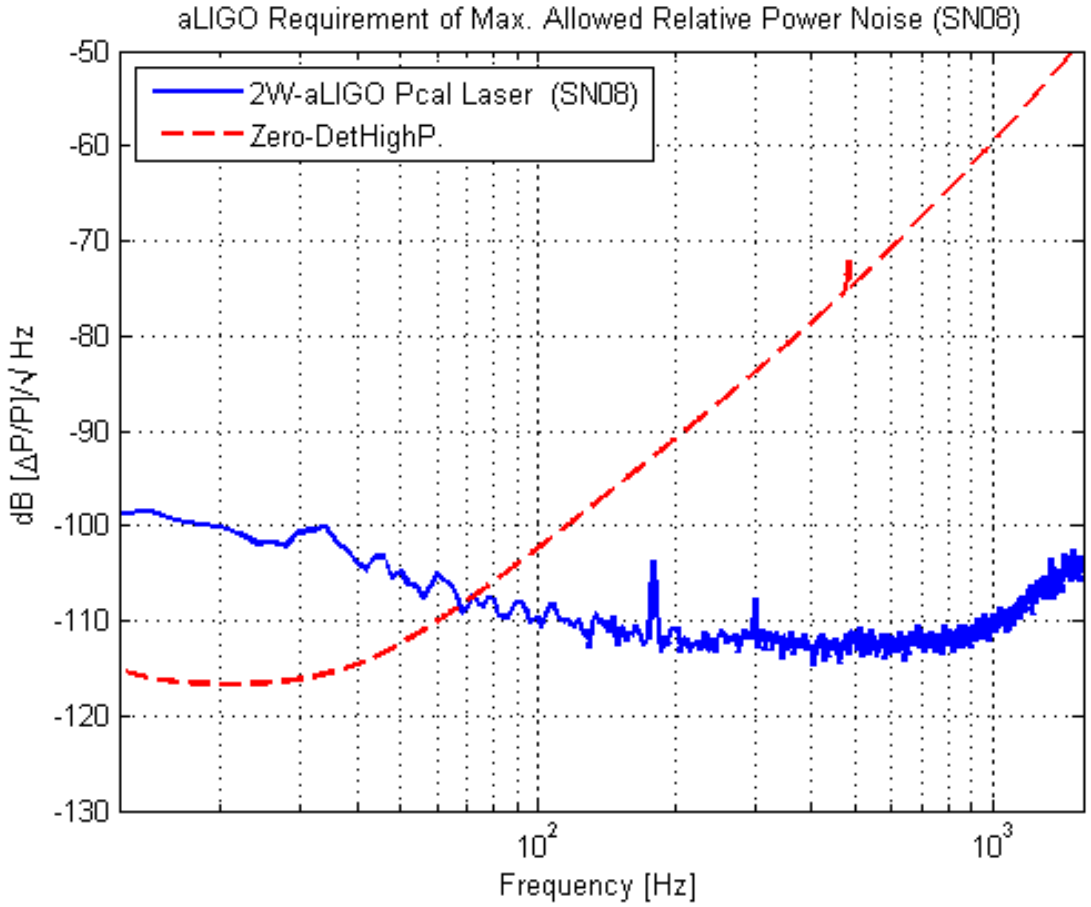

Figure 10 – RPN requirement sensitivity curve and measured RPN for Pcal laser SN08.

Displacement noise induced at harmonics of the Pcal modulation frequencies is required to be at least a factor of 10 below the anticipated displacement sensitivity. However, the amplitudes of the displacements induced by power fluctuations decrease with the square of the modulation frequency. Thus the requirement for the ASD of the laser power spectrum for harmonics is given by

$$\frac{\Delta P(nf_0)}{\Delta P(f_0)} = \frac{n^2}{10\,SNR}\frac{h(nf_0)}{h(f_0)} \qquad (6)$$

where SNR is the signal to noise ratio of the injected modulation at frequency f_0 with respect to the strain sensitivity curve $h(f_0)$ and n is the ratio of the harmonic frequency to that of the fundamental. Equation (6) is plotted in Figure 11 for the first three harmonics and for both the "zero detuning, high power" and "no SRM" configurations.

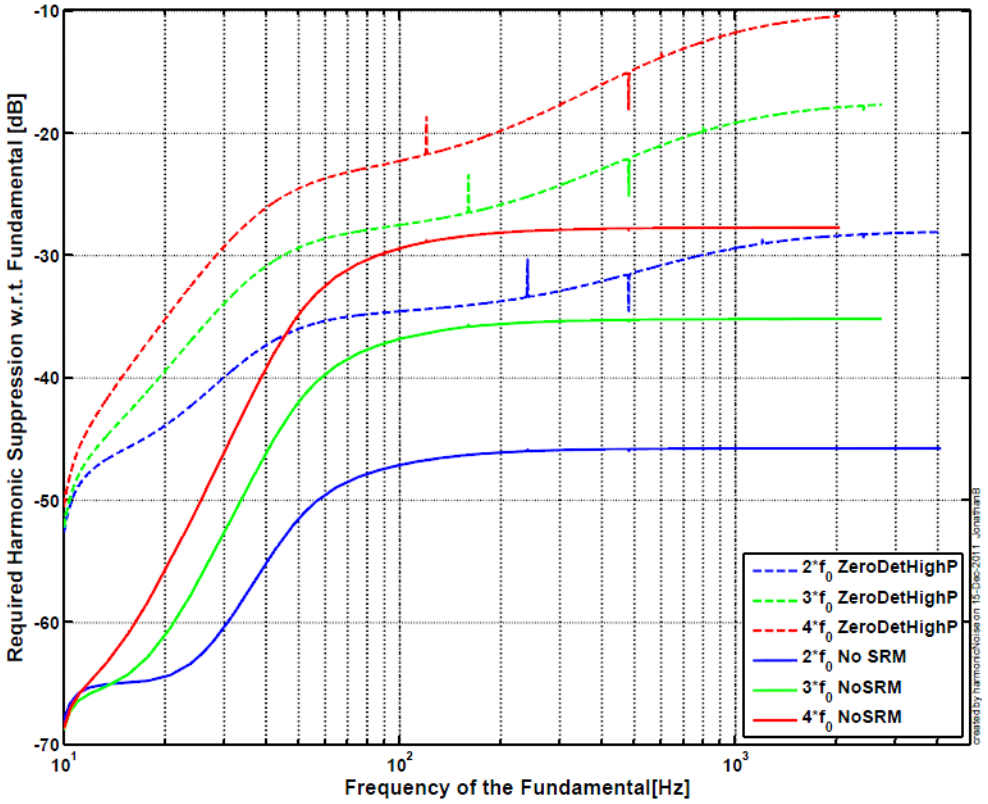

Figure 11 – Maximum allowable relative harmonic noise for the first four multiples of the frequency of the fundamental for both the "no SRM" and "zero-detuning, high power" configurations.

Suppressing both the power modulation at harmonics of the Pcal fundamental frequencies and inherent laser power fluctuations will require a power stabilization servo. We refer to this servo as the *Optical Follower* servo because we intend to inject the desired sinusoidal waveforms at the error point of the servo so that the servo will impress these waveforms on the modulated output power. See "Overview of Photon Calibrator Electronics" (LIGO-T1100556) for a more detailed discussion of this noise suppression servo.

2.4 UTC Synchronization

All excitations shall be independently and directly synchronized to UTC via GPS. See "Overview of Photon Calibrator Electronics" (LIGO-T1100556) for a full discussion of timing synchronization with UTC.

2.5 Laser Wavelength

There are two criteria for choosing the wavelength of the Photon Calibrator laser. First, the wavelength must be sufficiently distant from the interferometer laser wavelength to prevent noise

from scattered light coupling into the interferometer signals. We assume that the wavelengths must be separated by at least 0.3 nm to be outside the nominal tuning range of the NPROs that dictate the frequencies of the aLIGO PSLs. Second, we want to maintain high reflectivity on the HR coatings of the ETMs.

2.6 Continuous Excitation lines

Each Pcal shall operate continuously, simultaneously inducing periodic displacements of the ETMs at several frequencies. See "Overview of Photon Calibrator Electronics" (LIGO-T1100556) for a detailed discussion of how these excitations are implemented.

2.7 Swept-Sine Measurements

The Pcals shall be capable of performing swept sine measurements of the interferometer length response from 10 Hz to 1 kHz in less than 1 hour with coherence of 99% or better using CDS software.

2.8 Reliability

Mean Time Between Failures (MTBF) for out-of-vacuum components, including lasers and electronics, shall be at least 10,000 hours. The Pcals do not include active in-chamber components. See Section 8, "Failure Modes and Hazards," for a discussion of the reliability of the Pcals.

3 In-Vacuum Systems: Beam Paths and Periscopes

For aLIGO, the main interferometer beams will be situated as shown in **Error! Reference source not found.**. The ETMs are displaced by 20 cm horizontally to either side of the beam tube centerline and sit 8 cm below it. Because of the locations of the Optical Lever vacuum windows and receiver pylons, the Pcal transmitter pylons are located such that the Pcals transmit across the beam tube centerlines to reach the ETMs. Figure 12 shows the location of the Pcal and Optical Lever pylons for the L1 Y-end, which is typical of all end stations.

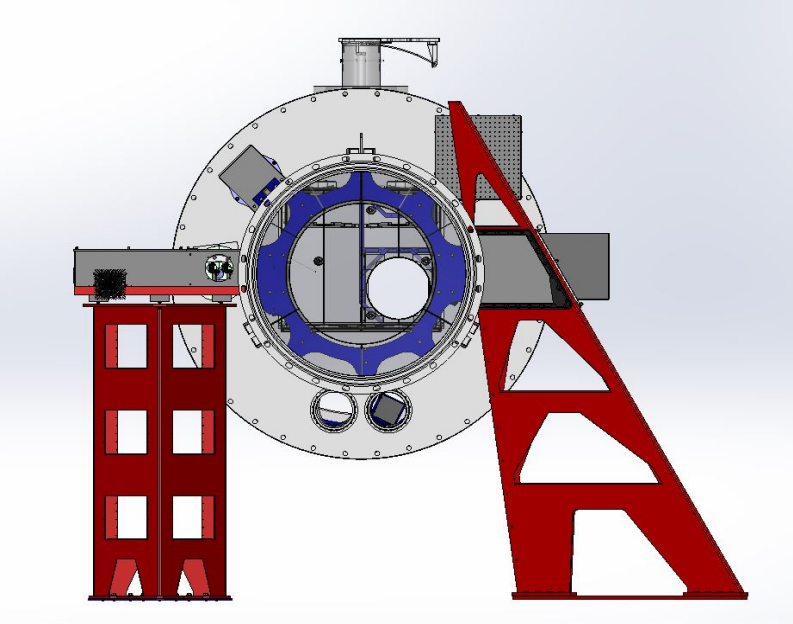

Figure 12 – View of L1 ETMX, looking from the corner station. The Pcal transmitter pylon is on the left with the Pcal camera housing just above it. The tall Optical Lever receiver pylon (which also houses the Pcal receiver module) shown on the right.

The "handedness" of the six Pcal configurations is tabulated in

Table 2. The layout of the Pcal transmitter module has been designed to easily switch between a right-handed and left-handed configuration by simply rotating two mirror mounts.

Table 2 – Handedness of Pcal modules, facing the HR surface of the ETM

Interferometer	Arm	Transmit side	Receive side	DCC#
H1	X	L	R	D0901468
	Y	R	L	D0901467
L1	X	L	R	D0901465
	Y	R	L	D0901464

3.1 Beam Paths and Periscopes

To achieve the required accuracy for the aLIGO Pcals, the Pcal beams must be precisely located on the ETMs at positions that minimize bulk elastic deformation of the ETMs. In aLIGO, folded Arm Cavity Baffles, with apertures just 4 mm in diameter larger than that of the ETM, are located upstream of the ETMs. These baffles preclude directing the Pcal beams directly onto the surfaces of the ETMs. The aLIGO Pcals thus use input periscopes that direct the Pcal beam toward the axis

of the beam tubes to decrease the angle of incidence on the ETMs and reduce interference with the Arm Cavity Baffles. In addition, for aLIGO the Pcal beams that reflect from the ETMs will be collected by in-vacuum periscopes and directed out of the vacuum system for continuous monitoring. This is in contrast to the iLIGO and eLIGO systems, which just let the reflected beams scatter off of the walls of the beam tube manifolds. Collecting the reflected beams will enable monitoring of the optical efficiency from the transmitter module output to the power reflected from the ETM and obviate the need for the in-chamber measurements that have proven necessary at the ends of the S5 and S6 science runs.

The in-vacuum periscopes will be mounted on a single compression ring that is similar to the design that the AOS system uses to mount baffles inside the beam tube manifolds.

Two baffles are positioned between the Pcal viewports and the ETMs (see LIGO-T0900269 for more information). They are the Cryopump Baffle, shown in Figure 13, and the Arm Cavity Baffle, shown in Figure 14.

A bird's-eye view of the LHO Y-end Pcal beam paths is shown in Figure 15.

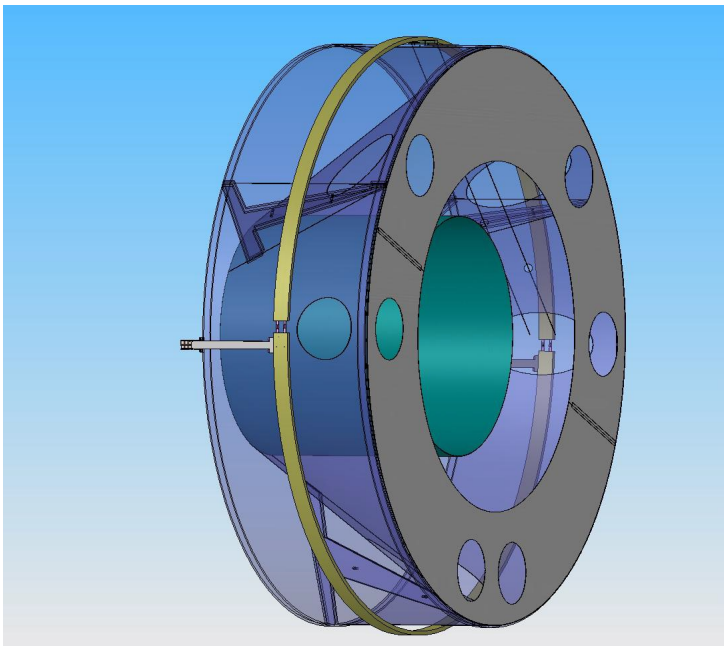

Figure 13 – Cryopump baffle positioned near viewports of H1 and L1. Holes in the baffle allow for Pcal beams, Optical Lever beams, and cameras to have access to the ETM.

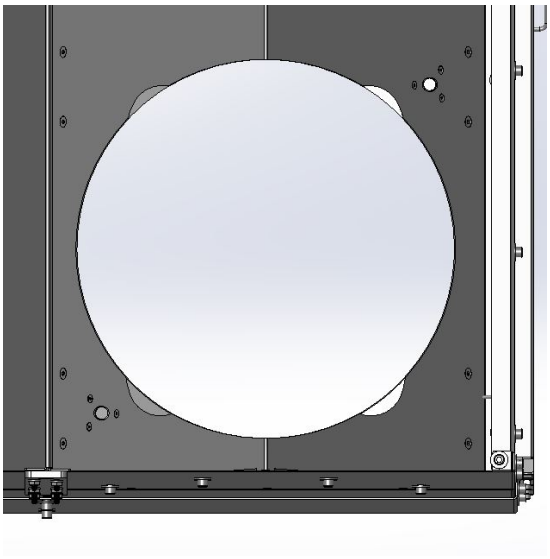

Figure 14 – Arm cavity baffle that is positioned in front of each ETM. The four "mouse ear" cutouts provide minimal clearance for the two Pcal beams.

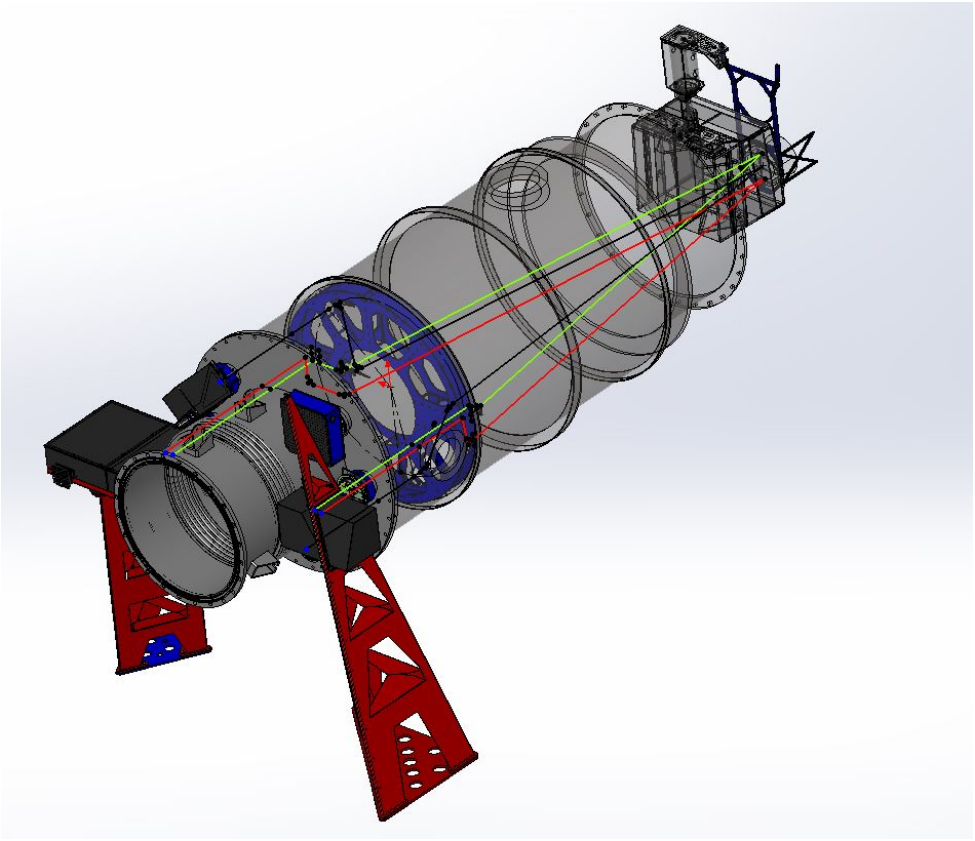

Figure 15 – Optical layout at the X-End Station. The figure shows the position of the Pcal transmitter module (square box to the left of the vacuum tube), and the Pcal receiver module that is mounted in the Optical Lever receiver pylons.

3.1.1 H1 and L1

Figure 16 and 17 illustrate the in-vacuum beam paths. Two horizontal beams leave the transmitter module and use in-vacuum periscopes to reach the ETM. All Pcals inject two beams that are horizontally displaced by 1.5" to either side of the center of the Pcal viewport. Both beams are vertically displaced by 1.24" above the viewport centerline such that the beam that will be directed to the upper spot on the ETM propagates horizontally from transmitter to receiver modules. The other beam, the beam that starts farthest from the beam tube manifold centerline, is directed down by an input periscope, then propagates horizontally to the ETM and the receiving periscope which directs it back up to the level of the upper beam (1.24" above the viewport centerline) and out of the vacuum system. All Pcal beams, input and output, propagate into and out of the vacuum system parallel to the beam tube centerline to or from the in-vacuum periscopes (see Figure 17).

All in-vacuum mirrors are 2" in diameter with HR coatings for 45 deg. incidence. All turning mirrors are in fixed mounts, with only azimuthal and a slight pitch adjustment, except the four periscope mirrors closest to the ETMs (one for each input beam and one for each output beam) that will utilize the standard aLIGO Siskiyou adjustable mounts.

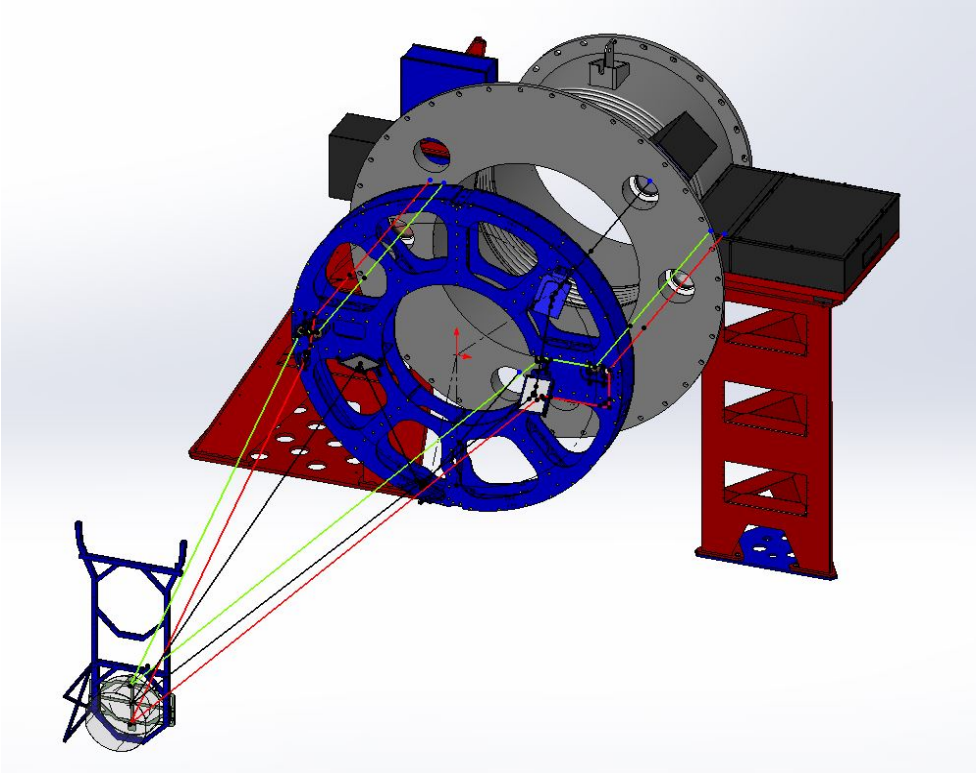

Figure 16 – In-Vacuum optical Paths of Pcal beams (green and red) and Pcal camera and optical lever (black) of H1, L1 Photon Calibrator Beams through the Pcal in-vacuum periscope.

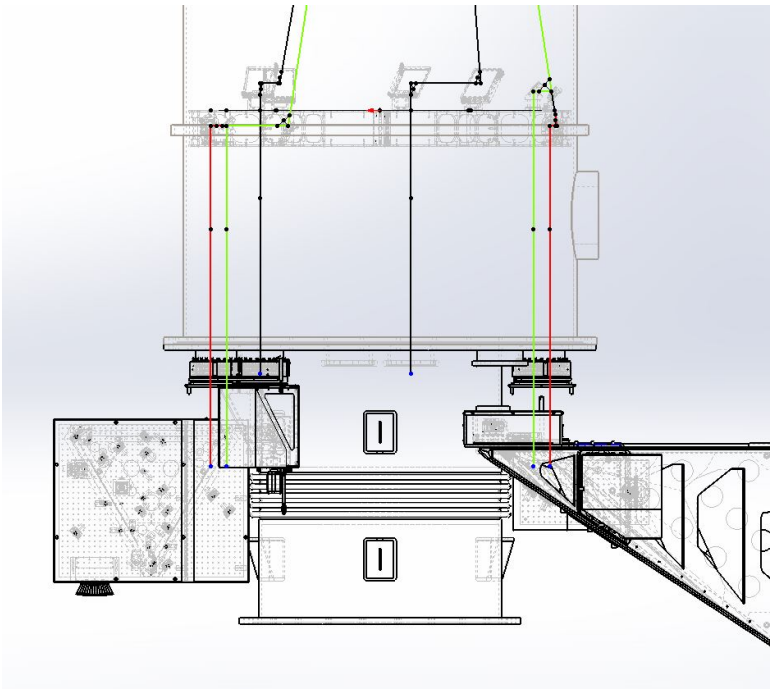

Figure 17 – H1X Pcal beams (red/green) entering from left and exiting from right at X-End Station, from a bird's-eye view. The black beam to the left is the Pcal camera view path and the black beam to the right is the ETM camera view path.

3.2 Beam Alignment and Localization

For iLIGO and eLIGO, the Pcal beams were aligned and located by viewing the light scattered from the ETM by the ETM cameras. The light emitted by the OSEMs was used for alignment fiducials and the HR surface of the ETM scattered enough of the Pcal light that the beam spots could be seen, as shown in Figure 18.

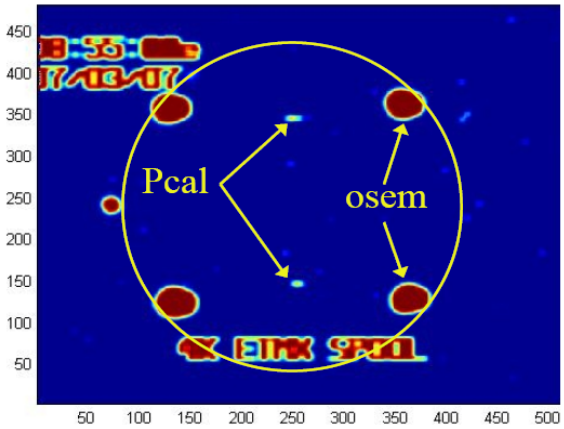

Figure 18 – BSC chamber camera view of ETMX showing the light from the OSEMs as well as the light scattered from the two photon calibrator beams.

For aLIGO, the Pcal lasers will be a factor of four more powerful, but we expect the ETM surfaces to scatter less light. Furthermore, we are striving for better localization of the Pcal beams on the ETM surfaces, ±1 mm accuracy.

3.2.1 Initial Alignment

The fold mirrors and periscope assemblies will be pre-aligned in the optics labs at the observatory sites before installation in the vacuum envelopes. Then, the beam paths will be pre-aligned using the ETM alingment target (see Figure **19**) mounted to the ETM suspension frame as shown in , to roughly locate the beams on the ETM surface by adjusting the final turning mirrors on the input periscopes.

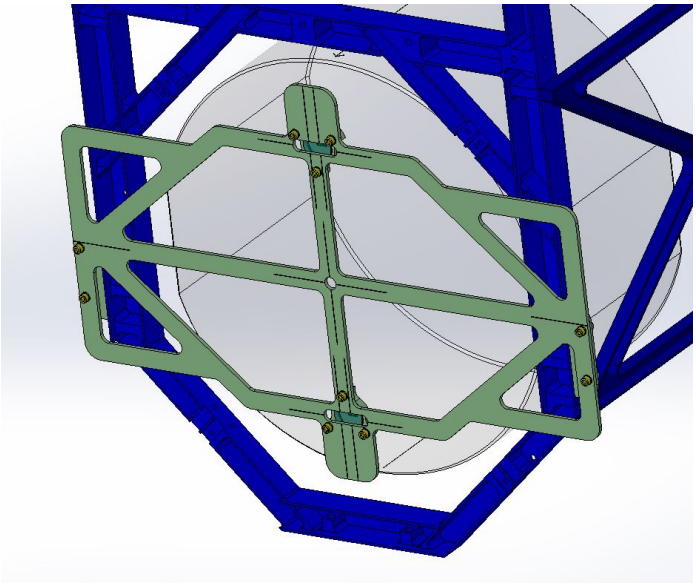

Figure 19 **–Pcal alignment target mounted to ETM suspension frame. Small optics mimic the ETM surface and are located at the optimal locations of the Pcal beams.**

3.2.2 Final Alignment

Final alingment of the Pcal beams through the vacuum system will be made using the Pcal beam localization system. The out-of-vacuum components of this system consist of the Pcal viewport camera hardware shown in figure 20 and image analysis software that provides the error in beam placement on the ETM. The in vacuum components are the camera view periscope mirrors mounted on the Pcal in-vacuum periscope which provide an optical path from the viewport to the ETM (see figures 16 and 17).

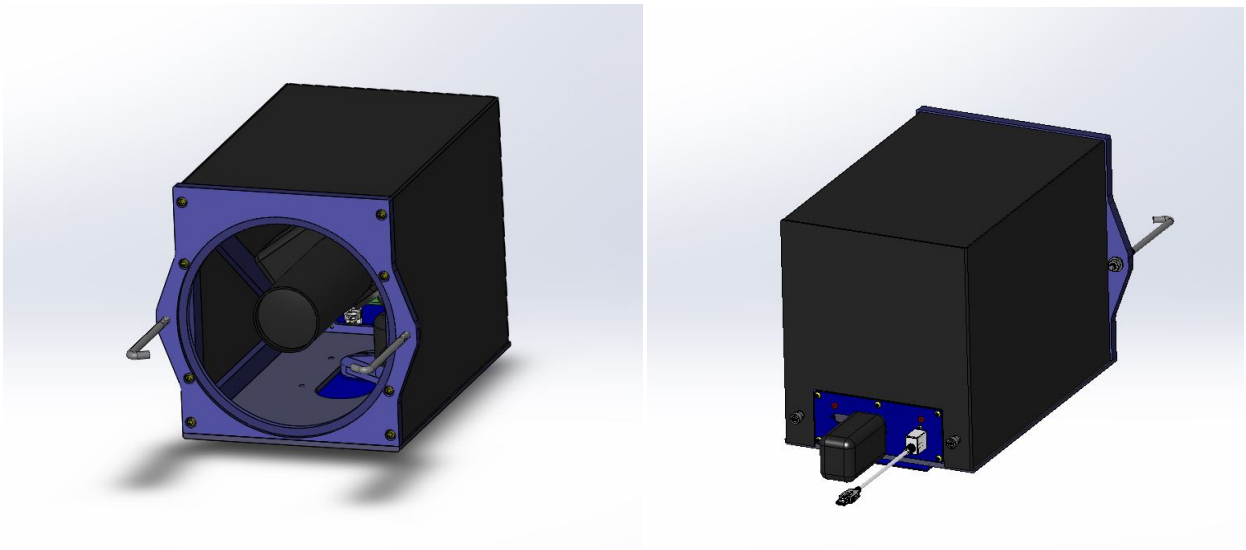

Figure 20 – Pcal viewport camera housing design (D1400181) with Nikon DSLR camera mounted inside. The Nikon UT-1 module protruding from the camera housing's electrical panel provides Ethernet connectivity between the camera and the Image analysis software.

3.2.2.1 Beam Localization Image Analysis Software

PCAL image analysis is a matlab script that uses photographs from the PCAL cameras to determine the location of artifacts on the test mass (e.g. PCAL beam spots) by using known parameters of the test mass physical dimensions and user inputs to form transformation operations that ferry coordinates between the image basis in pixels and the test mass basis in physical length units. The test mass basis is the x-y Cartesian coordinate basis that lies on the face of the test mass with the origin in the center and the y-axis parallel to the flat edge (not the face) of the test mass.

First, the image is loaded into matlab as an RGB, 3-layer pixel matrix and the image is displayed to the user. The user then carefully selects three points along the flat of the test mass: the upper-most point, the midpoint, and the lower-most point of the flat, and feeds the pixel coordinates to the script. In addition to three points along the test mass flat, the user must choose an arbitrarily large number (typically 12) of points along the curved edge adjacent to the flat, and likewise feed the pixel coordinates to the s script.

The script then does a linear fit on the three points along the flat edge to determine the "axis rotation angle", and this result can be used to form a rotation matrix that can correct for the tilt of the camera. Similarly, the script uses the points long the curved edge and fits them to an ellipse, and this resulting ellipse is used to form the metric used to translate between distances in pixels on the image to distance in physical units on the face of the test mass.

4 Transmitter Module

The transmitter module includes the laser, AOM, internal power sensor, and optical components necessary to generate the two power-modulated Pcal beams. All components are mounted on a 2" thick breadboard that will be mounted to the Pcal transmitter pylon, with a flexible bellows connecting its output aperture to the aperture of the viewport protector assembly. A schematic diagram of the optical configuration of the transmitter module is shown in

Figure 21.

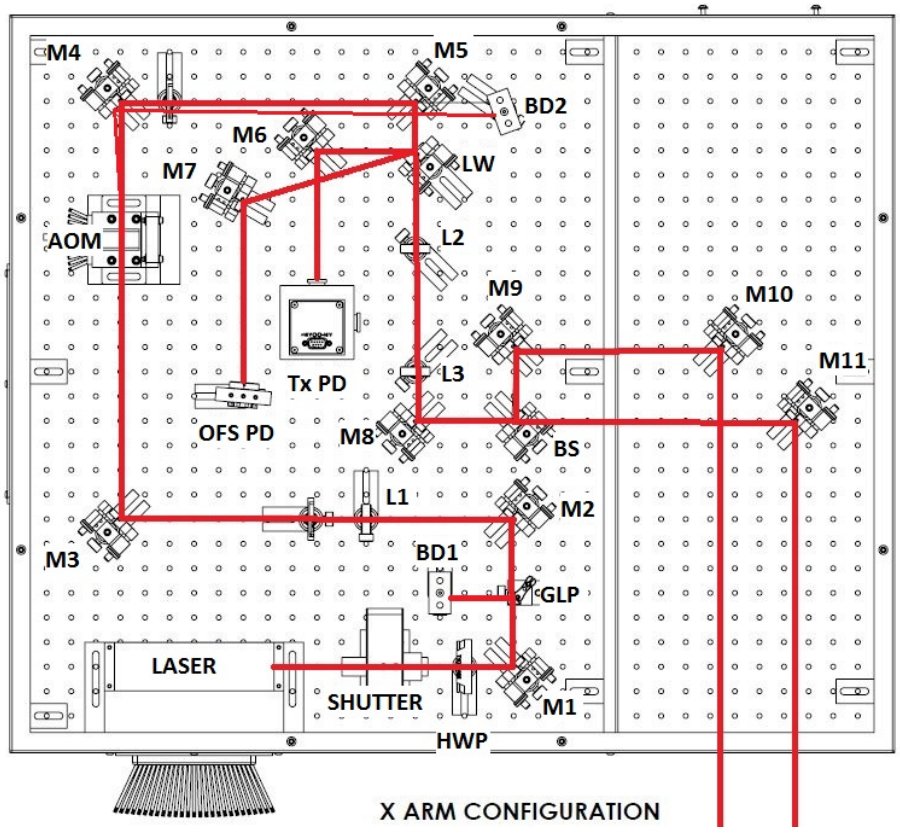

Figure 21 – Layout of Pcal transmitter module optical components.

4.1 Laser

Each transmitter module will contain a laser. The laser will be a 2W, continuous wave, 1047 nm Nd:YLF laser. This wavelength was chosen because it continues the calibration history of the Gold Standard and Working Standard from NIST which used 1047 nm light as well. The laser will be in continuous operation during a science run.

The aLIGO Pcal transmitter modules will also contain a remote-controlled mechanical laser shutter. Additionally, a feature of eLIGO that will be reused in aLIGO is a slow channel interface that allows the laser power to be turned on or off as necessary, remotely. See "Overview of Photon Calibrator Electronics" (LIGO-T1100556) for details.

4.2 Acousto-Optic Modulator

During iLIGO and eLIGO, the Pcals used ISOMET 1205C-843 AOMs and ISOMET 230 Series Analog RF Drivers. This RF driver model was discontinued so the ISOMET 532C-2-B, which includes a voltage bias adjust, will be used instead. This AOM driver will run at 80 MHz and generate about 1.3 W of RF power during operation. We will use the ISOMET 1205C-843 modulators for aLIGO

Control of the input signal into the AOM is discussed in "Overview of Photon Calibrator Electronics" (LIGO-T1100556).

4.3 Internal Laser Power Sensors

The aLIGO Pcals use internal power sensors in both the transmitter modules and the receiver modules to continuously monitor the modulated power waveform. These power sensors use InGaAs photodetectors with integrated pre-amplifiers that are mounted to 2" diameter integrating spheres (see

Figure 22). These are similar to the power sensors that were used in the eLIGO Pcals and found to be extremely stable (with a fraction of 1% over 18 months).

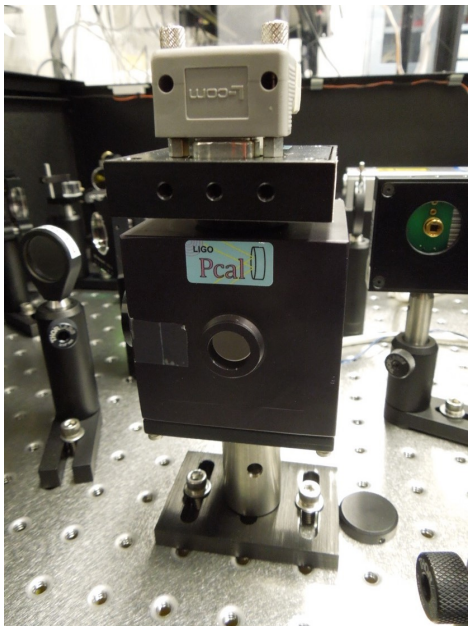

Figure 22 – Transmitter's Internal Photodetector and 2 inch Integrating Sphere

The internal power sensors will be directly calibrated by one of the Working Standards (see Section 6).

4.4 Physical and Environmental Monitors

A temperature sensor will be installed within the Pcal transmitter module enclosure to facilitate investigations of correlations with temperature variations and to give advance warning of changes in internal conditions.

4.5 Breadboard

The Pcal transmitter module will incorporate a 36” x 30” x 2” thick optical breadboard with ¼”-20 tapped holes on 1” centers.

4.6 Enclosures

The beam path of the Pcals will be entirely enclosed to ensure the safety personnel inside the VEAs and the integrity of the calibration. Both the transmitter and receiver modules will be completely enclosed with painted sheet metal enclosures similar to what was used for eLIGO (see Figure 23).

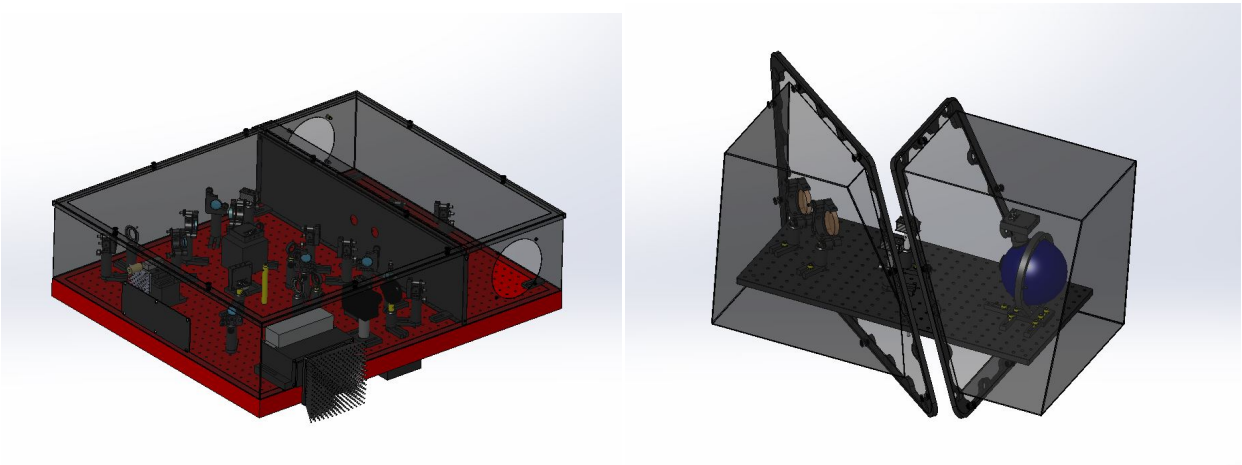

Figure 23 – aLIGO Pcal Transmitter (left) and Receiver (right) modules with enclosures shown in transparent.

4.7 Viewport Protectors

Viewport protectors, provided by AOS, will be installed on transmitter, receiver and camera housing viewports. These protect the viewport glass when work is ongoing inside the Pcal enclosures.

4.8 Transmitter Module Pylon

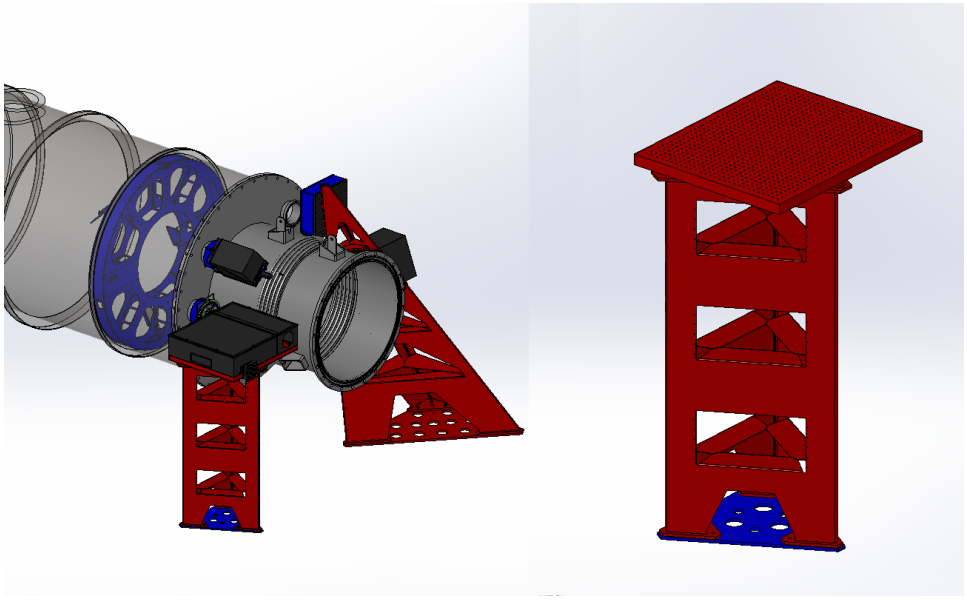

Figure 24 – Solidworks design of Pcal transmitter module pylon with breadboard (Right). The locations of the Pcal and Optical Lever pylons are show in the view on the left.

The transmitter module pylons are composed of 306 stainless steel sheet that is folded and welded in the manner developed for the Optical Lever pylons. The rectangular openings are sized to allow mounting of the Pcal electronics modules in 19" rack format. These include the laser power supply and AOM driver, power supplies for transmitter and receiver module components, signal conditioning boxes, and interlocks for access control.

The base of the pylon will be bolted to a grout plate that will be leveled, then bolted and grouted to the floor of the VEA. The pylon and breadboard can be seen in plan view in Figure 24.

5 Photon Calibrator Receiver Module

The aLIGO Pcals will also measure the power of the Pcal laser beams downstream of the ETM – outside the vacuum envelope, inside the Pcal receiver module. Both beams are directed to a single power sensor. For absolute power calibration the receiver power sensor is swapped with a working standard using alingment blocks fixed to the receiver breadboard. The receiver breadboard layout can be seen in Figure 25.

5.1 Internal Power Sensor

The receiver module internal power sensor will be similar to the power sensor used for the transmitter module. The two Pcal beams will be directed into the entrance aperture of the power sensor's integrating sphere at near-normal incidence. The receiver module will also contain a mirror on a removable kinematic stage to accommodate the Working Standard for calibration measurements (see Figure 25).

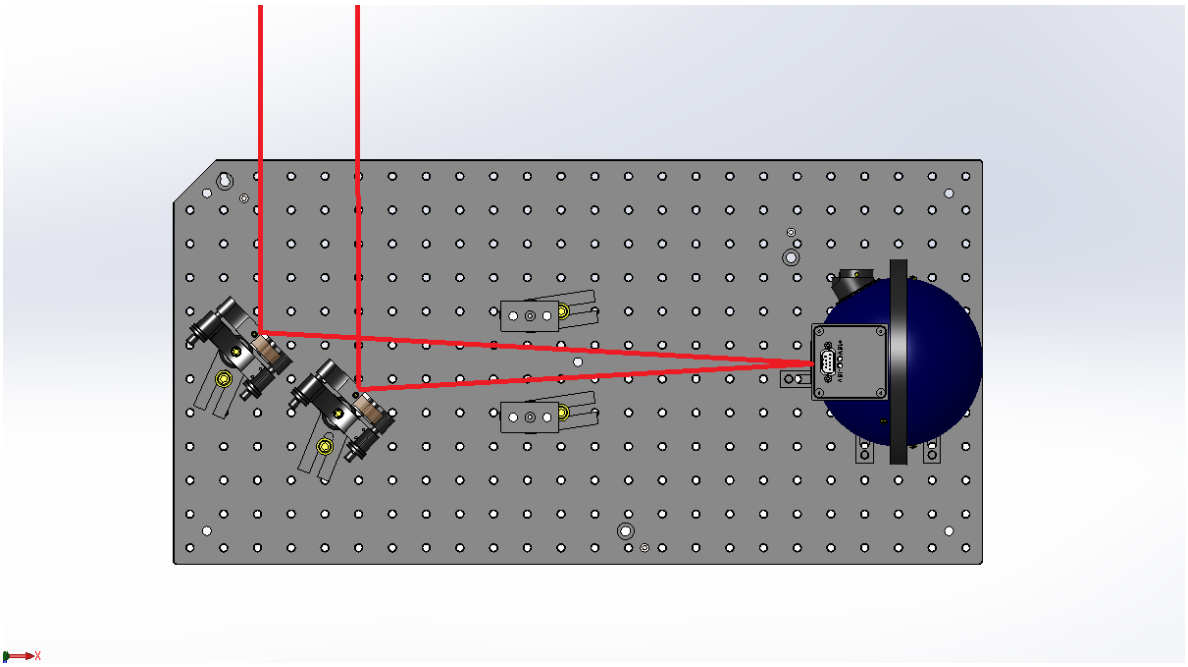

Figure 25 – Receiver Module Layout (LIGO-D1200216).

5.2 Calibration of the Photodetector

The receiver module's power monitor will be calibrated about as often as the transmitter module's power monitor. Comparison of the transmitter and receiver module power sensors will enable assessment and tracking of changes in the transmissivity of the optical path between the transmitter and receiver modules – the vacuum windows and the ETM HR surface. This is to ensure that the read-back at the receiving point is stable and accurate. In addition, calibration staff may elect to use both photodetectors equal agents for the interferometer calibration.

Calibrating the receiver photodetector may be done by either the local Working Standard or by comparing the response of the transmitter read-back and the receiver read-back for a defined period.

5.3 Receiver Module Pylon

The Pcal receiver modules will incorporate 12" x 18" x ¾" thick aluminum breadboards that will be mounted in an opening in the pylons for the Optical Lever receiver modules. The breadboards will have ¼"-20 tapped holes on 1" centers. The Pcal receiver module will be covered on all sides with painted aluminum sheet metal housing that will be bolted to the Optical Lever receiver pylon. A viewport protector will be installed on the viewport window and a flexible bellows will connect the Pcal receiver module enclosure to the viewport protector.

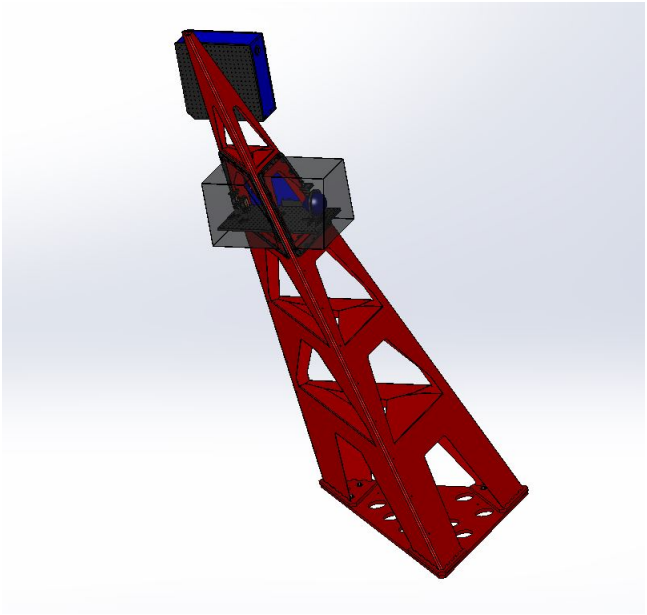

Figure 26 – Photon Calibrator receiver breadboard mounted inside of the Optical Lever receiver pylon with enclosure surrounding the module.

6 Absolute Laser Power Calibration

The absolute power calibration strategy described in Section 2.1 relies on a Gold Standard that is calibrated by NIST and Working Standards that are used to calibrate the Pcal power sensors located inside of the transmitter and receiver modules.

6.1 The Gold Standard Laser Power Sensor

The power sensor that is sent to NIST for absolute power calibration is referred to as the Gold Standard. NIST calibrates LIGO's Gold Standard according to guidelines specified in NIST document SP 250-75. LIGO donated a 1047nm laser to NIST for use in calibrating the eLIGO Gold Standard. This significantly reduces the cost to LIGO for the NIST's calibration services. During eLIGO, NIST achieved a calibration precision of $\frac{2\sigma}{\mu} < 1\%$. The Gold Standard will be sent to NIST annually for calibration. The cost is approximately $8000.00 per calibration.

Both the Gold Standard and the Working Standards use 4" diameter integrating spheres manufactured by Labsphere in North Sutton, NH (model 3P-040-LPM-SL) with Spectralon surface coatings, 1" diameter entrance apertures, and ½" diameter detector apertures.

Receiver module packages sold by Labsphere are used. The photodetectors for these packages are manufactured by Electro-Optical Systems (model IGA-030-TE2-H), of Phoenixville, PA, and are mounted to the spheres. These receivers use hermetically-sealed InGaAs photodetectors mounted on thermo-electric coolers. We operate them at –10°C. These receivers are operated unbiased, in "photovoltaic" mode. Their photocurrents are converted to voltages by fast current amplifiers sold by Keithley Instruments of Cleveland, OH (model 428 PROG). The outputs are read and digitized by Keithley Model 2000 digital multi-meters. The Working Standard system, which is identical to the Gold Standard system, is show in Figure 27.

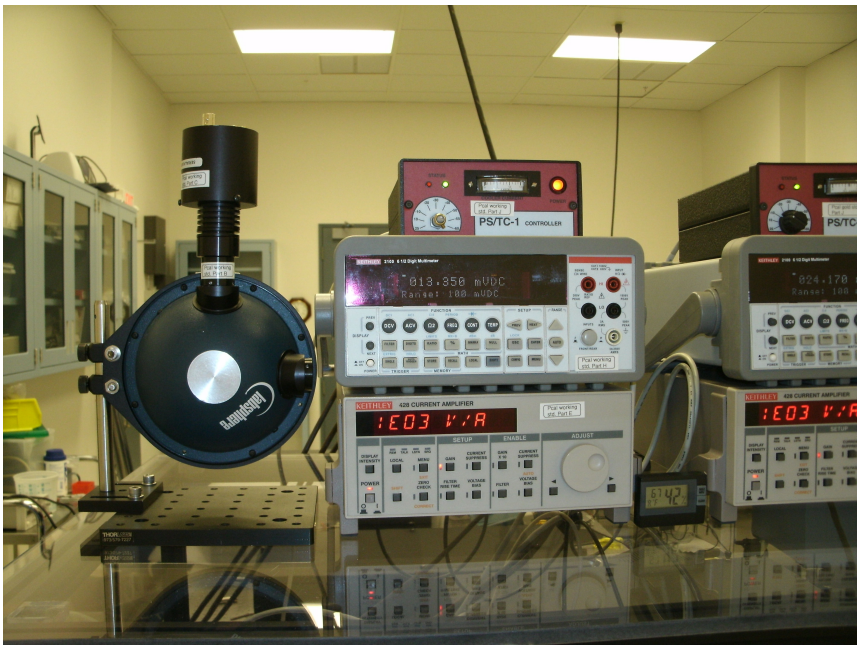

Figure 27 – eLIGO Working Standard power sensor including the integrating sphere, photo-receiver module, fast current amplifier, digital multimeter, and power supply/thermo-electric cooler controller.

Using the Gold and Working standards since 2007, we have found the receiver module manufactured (packaged) by Labsphere to be less stable and less reliable than photo-receiver modules manufactured and sold by Elecro-Optical Systems (EOS). These modules use the same detector package as the Labsphere receivers, but with better-engineered heat sinking and an integrated transimpedance pre-amplifier that uses a single operational amplifier. During eLIGO, the Pcal systems at both LHO and LLO used internal power sensors that incorporated these EOS receivers. For aLIGO, we plan to switch to the EOS receiver modules on both the Gold and Working standards. We will likely also operate the receivers at room temperature, reducing the complexity by eliminating the thermoelectric cooler temperature stabilization control loop and thus improving reliability, as we have had several failures of the power supplies and temperature stabilization controllers. InGaAs is sufficiently insensitive to temperature variations at this wavelength and the variations in ambient and sphere temperatures are small enough that operating at room temperature should not introduce significant changes in the absolute calibration.

6.2 The Working Standard Laser Power Sensors

Calibrating the Pcal internal power sensors (in both the transmission and receiver modules) for absolute power calibration requires travel to the end stations with a NIST-traceable standard, at both LHO and LLO. Rather than taking the Gold Standard to the end stations, we establish derivative standards called *Working Standards*. During eLIGO, there was only one Working Standard and we shipped it periodically to LLO to calibrate the L1 interferometer. During aLIGO, there will be two Working Standards, both of which will be calibrated periodically to the Gold Standard. This will allow us to increase the frequency of calibrations of the power sensors at the end stations at LLO and reduce the number of times that Working Standards need to be shipped between sites, saving about $1,000 in round trip shipping costs.

7 Calibration Procedures

7.1 Calibration of the Working Standard

The Gold Standard calibration (from NIST) is transferred to the Working Standard using the optical configuration shown schematically in Figure 28.

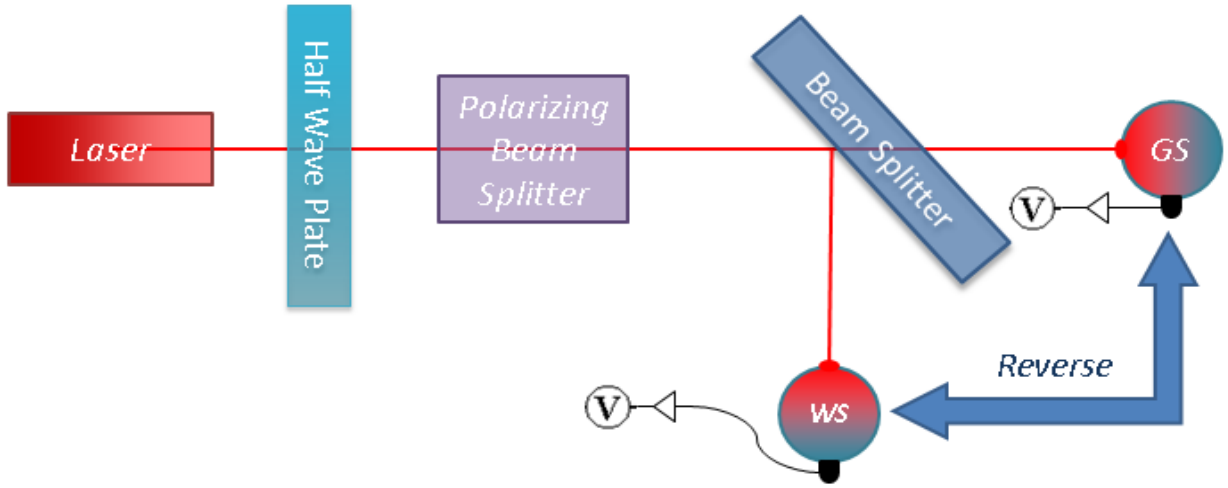

Figure 28 – Working Standard-Gold Standard calibration setup

A photograph of the actual setup, located in one of the optical laboratories at LIGO Hanford Observatory, is shown in Figure 29.

The laser used in this setup is identical to the lasers that are used in the Pcal transmitter modules. The beamsplitter is a 2" diameter, fused silica, 3° wedge with a nominal 50% reflectivity. The detailed procedure for transferring the calibration can be found in LIGO-T1100315. In summary, each of the two sensors measures light at one of two ports of the beamsplitter (transmission or reflection), data are recorded simultaneously, and then the locations of the power sensors are swapped (reversed) and the measurements are repeated.

The relative calibration of the Working Standard is calculated as follows:

$$\frac{Working\ Standard\ Responsivity}{Gold\ Standard\ Responsivity} = \sqrt{\frac{WS_{refl}R}{GS_{trans}T}\frac{WS_{trans}T}{GS_{refl}R}} = \sqrt{\frac{WS_{refl}WS_{trans}}{GS_{trans}GS_{refl}}} \qquad (7)$$

where the subscripts *refl* and *trans* indicate the location of the sensor for a particular measurement and T and R are the power transmissivity and reflectivity of the beamsplitter, respectively. T and R do not need to be measured independently they appear in both the numerator and denominator of Equation (7) and therefore cancel.

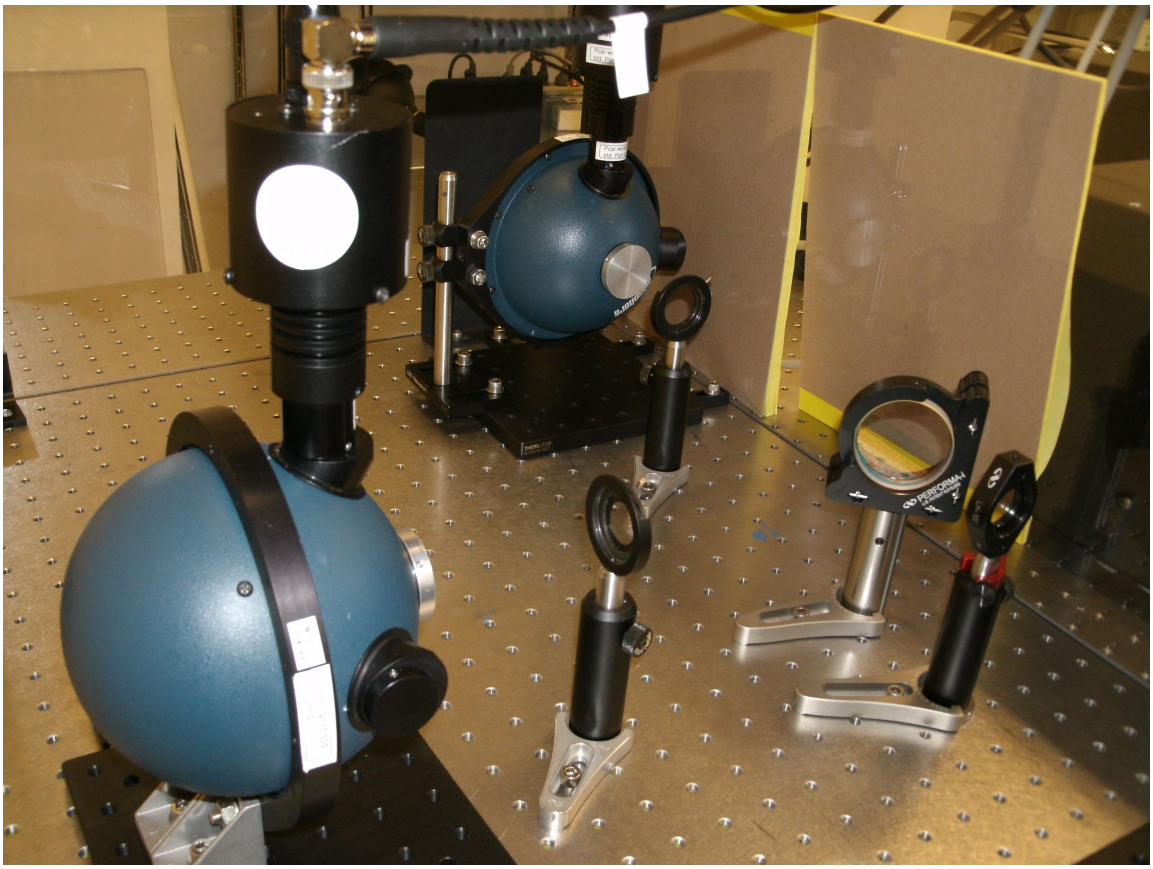

Figure 29 - Photo of optical setup for transferring the NIST calibration from the Gold Standard (left, foreground) to the Working Standard (right, background).

7.2 Calibration of Transmitter and Receiver Module Power Sensors

7.2.1 Frequency of Calibration

Each power sensor will be calibrated at least once every 2 months using the local Working Standard.

The calibration procedure that was used during eLIGO is detailed in the Photon Calibrator Calibration Procedure (http://www.ligo-wa.caltech.edu/~michael.sakosky/PCALcal.html). This procedure compares the response of the Photon Calibrator internal photodetector with the response of the Working Standard at two different DC voltages injected into the excitation channel. The calibration formula, which is applied to each of the two Pcal output beams, is as follows:

$$\frac{\Delta \boldsymbol{Volts_{WS}}}{\Delta \boldsymbol{Counts_{PM}}}(DC) = \frac{Volts_{WS}(1\,Volt) - Volts_{WS}(0\,Volts)}{Counts_{PM}(1\,Volt) - Counts_{PM}(0\,Volts)} \tag{8}$$

Equation (8) indicates how the reading from the transmitter/receiver internal photodetectors ("$Counts_{PM}$") and the Working Standard ("$Volts_{WS}$") combine to form a "Box Calibration," as it was called during eLIGO. This result can be combined with the Gold Standard and Working Standard Calibrations to give the Pcal transmitter module output power in watts:

$$\Delta \boldsymbol{p_{Watts}} = \Delta \boldsymbol{Counts_{PM}} \frac{\Delta \boldsymbol{Volts_{WS}}}{\Delta \boldsymbol{Counts_{PM}}} \frac{Volts_{GS}}{Volts_{WS}} \frac{Watts_{NIST}}{Volts_{GS}} \quad (9)$$

The power sensor calibration in Equation (9) together with the transmissivity of the Pcal input window and reflectivity of the ETM coating is used to convert the internal power sensor signal to p_0, the amplitude of the modulated laser power Equation (1).

8 Failure Modes and Hazards

8.1 Internal Photodetector Fails

This occurred during S6 in the Pcal transmitter module for ETMX on the L1 interferometer. The trend of the voice coil actuator calibration revealed the step in the calculated actuation coefficient when the receiver failed. For aLIGO, there will be two power sensors per Pcal system, one in the transmitter module and one in the receiver module. Continuous monitoring of the ratio of the signals from the two sensors will reveal a failure if one should occur. Calibration using the working standard will reveal which sensor changed it responsivity. Continuity of the interferometer calibration can be maintained by referring to the sensor that did not suffer the failure.

8.2 Gold Standard or Working Standard Fails

If this were to occur, one of the other standards could take the place of the failed standard and the continuity of the NIST calibration could be maintained by referring to the standards that did not suffer the failure. Note that for aLIGO we plan to have three calibration standards, the Gold Standard and one Working Standard at each observatory. Periodic cross-calibration of the standards and yearly calibration of the Gold Standard at NIST ensures the ability to identify a calibration standard failure.

8.3 Laser Fails

If a laser or entire Photon Calibrator system would fail, the interferometer calibration would still be maintained from the Photon Calibrator of the opposite arm of the interferometer. If the finesses of each arm are approximately equal, as they were during eLIGO, the interferometer cannot differentiate between actuation from either arm, so this failure would not be a critical concern. The only concern of this failure would be less power available for calibration, thus lowering the SNR of calibration lines and precision of the calibration.

8.4 Misalignment of Receiver-Side Periscope

If the receiver-side in-vacuum periscope would be misaligned and the beam no longer cleanly passes out the receiver viewport window, then that receiver system would no longer be operable until the next in-vacuum entry. In this case, we would rely on the transmitter side power sensor and other arm's Pcal system for the calibration. Additionally, because the wavelength of the Pcal laser is at least 0.3 nm away from the wavelength of the main interferometer laser, Pcal stray light introducing noise into the interferometer signals should not be an issue.

8.5 Misalignment of Transmitter-Side Periscope

If the transmitter-side periscope were to drift so that the beam spot would drift from its optimal position on the ETM by several millimeters or clip on another in-vacuum component, that Pcal system would be compromised. However, continuous monitoring of the beam positions on the ETM surface, each time the interferometer loses lock, for instance, would reveal changes in the input beam alignment. The alignment could be corrected by the steering mirrors located outside the vacuum envelope.

8.6 Damage to Viewport Glass

Viewport protectors will preclude physical access to the viewport glass during maintenance operations, as outlined in LIGO-T1000023. During normal operation, the viewport glass will be exposed to the interior of the transmitter and receiver modules which will be fully enclosed and the enclosure covers will be interlocked such that an alarm will sound if they are removed without authorized access to the Pcal modules. The only movable component inside the Pcal modules is the mechanical shutter inside the transmitter module and it will be located far from the viewport glass.

9 Required Drawings and Documents

9.1 Hardware Drawings/Bill of Materials

9.1.1 Transmitter Pylon (same for all ETMs, 6 required)

Pcal Transmitter Pylon Main Assembly (LIGO-D1000625)

9.1.2 Transmitter Module (same for all ETMs, 6 required)

Transmitter Module Main Assembly (LIGO-D1201072)

9.1.3 Receiver Module (same for all ETMs, 6 required)

Receiver Module Main Assembly (LIGO-D1300800)

9.1.4 Pcal Viewport Camera

Pcal Viewport Camera Housing Design (LIGO-D1400181)

9.1.5 In-Vacuum Periscope Structure (same for each ETM, except left-right symmetry, 6 required)

In-Vacuum Periscope Main Assembly (LIGO-D1200174)

10 Annex

10.1 Acronyms

μ - Mean

σ – Standard Deviation

1 PPS – 1 Pulse Per Second timing system

AOM – Acousto-Optic Modulator

AR - Antireflection mirror coating

BS - Beam Splitter

BSC – Basic Symmetric Chamber

CDS – Control and Data System

DAQ – Data Acquisition System

GS – Gold Standard

HR – High Reflectance mirror coating

HWP- Half Wave Plate

IFO - LIGO interferometer

ISC- Interferometer Sensing and Control

Pcal – Photon Calibrator

PM – Internal Power Monitor that is located inside of the Photon Calibrator box

ppm - parts per million

QWP – Quarter Wave Plate

RPN – Relative Power Noise

RMS – root mean square

SNR – Signal-to-Noise Ratio

WS – Working Standard

WSH – Working Standard Hanford

WSL – Working Standard Livingston

10.2 Relevant Documents

DCC references in italics refer to external documents.

Title	LIGO-DCC#:
Precise calibration of LIGO test mass actuators using photon radiation pressure	P080118
Accurate calibration of test mass displacement in the LIGO interferometers	P0900155
Photon Calibrator Upgrades Proposal	T070094
Photon Calibrator Conceptual Design Document	T070167
Photon Calibrator Response to Reviewer's Report	G070601
Photon Calibrator Design Requirements	T1100044
aLIGO Calibration White Paper	T1100122
Viewport Subsystem Preliminary Design Document	T1000023
Optimal calibration accuracy for gravitational-wave detectors (Lindblom)	*PRD-Aug 2009*[4]
NIST: Report of Calibration for First Photon Calibrator Calibration	T1000637
NIST Report of Special Test	T070246
Photon calibrator gold standard calibration at NIST - Report of Calibration (42110CA)	T1000189
NIST Measurement Services: cw Laser Power and Energy Calibrations at NIST	*NIST SP 250-75*[5]
aLIGO Photon Calibrator Errors due to Elastic Deformation	G1100332
eLIGO Photon Calibrator investigation: long term stability of DARM actuation	G1000254
Characterization of Photon Calibrator data from S6	G1000913
Photon Calibrator Investigations During S6	G1100189
AOS Pcal Technical Status - NSF 2011	G1100454
S6 V2 Calibration Review	T1100597
Controlling calibration errors in gravitational-wave detectors by precise location of calibration forces (paper)	P1100166
Controlling calibration errors in gravitational-wave detectors by precise location of calibration forces (poster)	G1100988
Photon Calibrator Budget Estimate	T1100643

[4] http://www.tapir.caltech.edu/~lindblom/Publications/86_PhysRevD_80_042005.pdf

[5] http://www.nist.gov/calibrations/upload/sp250_75.pdf